Two-dimensional crystalline phases of CF_3H adsorbed on graphite

K. Knorr and H. Wiechert
Institut für Physik, Universität Mainz, D-6500 Mainz, Federal Republic of Germany
(Received 8 June 1987)

Trifluoromethane, CF_3H, adsorbed on the (001) faces of exfoliated graphite has been studied by x-ray diffraction. An orientationally disordered, triangular, incommensurate high-temperature and an orientationally ordered low-temperature phase have been observed. In the low-temperature phase the molecules show staggered orientations; the lattice is uniaxially compressed. The coverage-temperature phase diagram has been derived. Above one monolayer bulk crystallization sets in.

I. INTRODUCTION

Monolayers of gases adsorbed on homogeneous substrates like the (001) planes of graphite are excellent examples of quasi-two-dimensional (2D) arrangements of matter. The phases and phase transitions of monolayers and submonolayers of the noble gases have been studied in detail with respect to the problem of 2D melting and of their commensurability to the corrugation of the substrate.[1] More recently, the adsorbed phases of nonspherical molecules like O_2 (Refs. 2–5), N_2 (Refs. 5–7), CF_4 (Refs. 8 and 9) have attracted experimental and theoretical interest. There, the orientations of the molecules introduce additional degrees of freedom and, in fact, orientationally disordered and ordered phases have been detected and described theoretically using different approaches, computer simulations,[10–13] Kosterlitz-Thouless-type models,[14] and various Hamiltonians, like Potts models[15] and anisotropic XY models,[16] depending on the symmetry of the adsorbate-substrate system.

For the present study we have chosen trifluoromethane CF_3H which is one of the simpler molecules which carries a permanent electric dipole moment and which is therefore well suited for the search of electrically ordered phases in 2D. Dielectric measurements on CF_3H adsorbed on BN indeed suggest a ferroelectric transition at about 50 K.[17] As far as shape and dimensions are concerned, CF_3H resembles closely its nonelectric counterpart CF_4, the 2D phases of which are known from diffraction[8] and specific-heat[9] experiments.

II. EXPERIMENTAL

The sample was a sheet of exfoliated graphite (Papyex, Carbonne Lorraine) of 0.63 g and 1 mm thickness. After outgassing at 1000 C under vacuum the substrate was introduced into the sample cell which is mounted to the cold plate of a closed-cycle refrigerator. The cell and the vacuum jacket of the refrigerator are partly made out of Be, 0.3 mm thick, in order to allow the passage of the x rays. The CF_3H gas, 99.8% pure, was introduced from the gas-handling system into the cell through a heated capillary. The gas-handling system is made out of steel tubing and reservoirs, bellow sealed valves, and metal-to-metal connections. It is equipped with a capacitance pressure gauge (MKS-Baratron, 100 mbar maximum).

For the diffraction measurements Cu $K\alpha$ ($\lambda = 1.542$ Å) radiation has been used emerging from the line focus of an x-ray tube, operated at 40 kV and 20 mA. The x rays are reflected from a vertically bent (002) graphite monochromator, pass through the sample, and enter a position-sensitive detector, as sketched in Fig. 1. In the scattering plane the scattering geometry is parafocusing. The sample is oriented in a way that the scattering vector lies in the sheet plane. As the graphite c axis is preferentially normal to the sheet plane, the graphite (002) intensity is strongly reduced. The detector covers 8 deg in the scattering angle 2θ. Most data have been collected with the detector centered at $2\theta = 23$ deg. The counting time was one or half an hour per run. The ratio of counting rates of the Bragg reflections to that of the background was about unity for the strongest 2D peaks and eight for the graphite (002) peak. For 2θ about 23 deg the 2θ resolution is 0.19 deg [full width at half maximum (FWHM)], it is mainly due to the finite thickness of the sample. The data have been reduced by subtracting reference data obtained with no gas in the cell. Warren line shapes based on Gaussian structure factors[18] have been fitted to the reduced spectra yielding values for the parameters of the fits: the peak height and 2θ position and the coherence length. Two further parameters characterizing the substrate have been determined once from fits to the strongest 2D peaks and held constant in the following: (i) the ratio of the randomly oriented part of the graphite to that part the (001) planes of which are preferentially aligned parallel to the sheet plane and (ii) the mosaic width of the latter part. Values of 0.6:0.4 and 16 deg [half width at half maximum (HWHM)] have been determined.

In total nine different quantities of gas have been introduced into the cell. Each of these coverages has been studied at typically 30 different temperatures. Whenever new gas was admitted to the cell, it turned out to be necessary to anneal the sample at about 150 K. The coverage ρ will be given in terms of molecules per three graphite hexagons. $\rho = 1$ corresponds to a perfect monolayer of a $\sqrt{3} \times \sqrt{3}$ 2D solid. For this calibration an adsorption isotherm ($T = 80$ K) has been measured with Kr where a substep near monolayer completion indicates the

transition from the completed $\sqrt{3}\times\sqrt{3}$ R 30° structure to the incommensurate triangular phase.[19]

III. RESULTS

Figure 2 shows two examples of diffraction profiles for $\rho=0.81$. At the higher temperature there is a single diffraction peak which splits at lower T. An additional weak peak at $2\theta=20.7$ deg appears at low T. Figure 3 shows the T dependence of the strong peak more closely. These data demonstrate that CF_3H adsorbed on graphite forms two different 2D crystalline phases. The 2D character is evident from the asymmetric shape of the Bragg peaks. The transition temperature between the two solid phases will be denoted by T_c, the melting temperature by T_s. From the experimental point of view T_s is defined as the highest temperature where 2D Bragg peaks could be observed. The dependence of T_c and T_s on the coverage ρ is shown in Fig. 4. For high ρ and T, ρ is corrected considering the finite 3D gas pressure in the cell. For $\rho>1$ sharp extra peaks of symmetric shape grow rapidly with ρ. They are attributed to 3D CF_3H crystallites since the peak positions agree with those of bulk CF_3H on which we performed a complementary powder diffraction study. Bulk CF_3H forms a single solid phase of presumably triclinic structure, but so far we have been unable to index the powder lines, let alone present a model for the arrangement of the molecules. We do not know of any other structure determination. The melting point is around 117 K since at that temperature bulk CF_3H is liquid on cooling and crystalline on heating, as can be seen from the diffraction patterns.

A. Cell dimensions

The signature of the high-temperature crystalline phase, stable between T_c and T_s, is a single 2D peak in the range 10 deg $<2\theta<38$ deg; hence a triangular structure is the natural guess. In order to facilitate discussion, the triangular structure is described in terms of a centered rectangular cell containing two molecules with the cell parameters a and b where $b=\sqrt{3}a$ or alternatively by the area A covered by one molecule, $A=\frac{1}{2}ab$. The strong peak of Figs. 2 and 3 is then identified as the triply degenerate line (11),(1$\bar{1}$),(02). The T dependence of A is shown in Fig. 5 for three coverages. Throughout the tri-

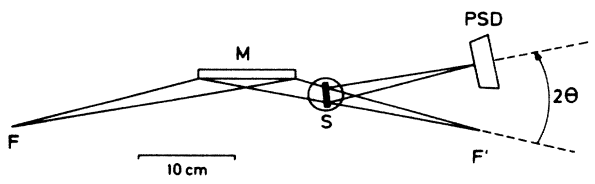

FIG. 1. Schematic drawing of the x-ray setup. Vertical line focus F and image F', vertically bent graphite monochromator M, sample S with the graphite c axis lying in the scattering plane, position sensitive detector PSD. The actual width of M is 12 mm, the width of the beam at S, 1 mm.

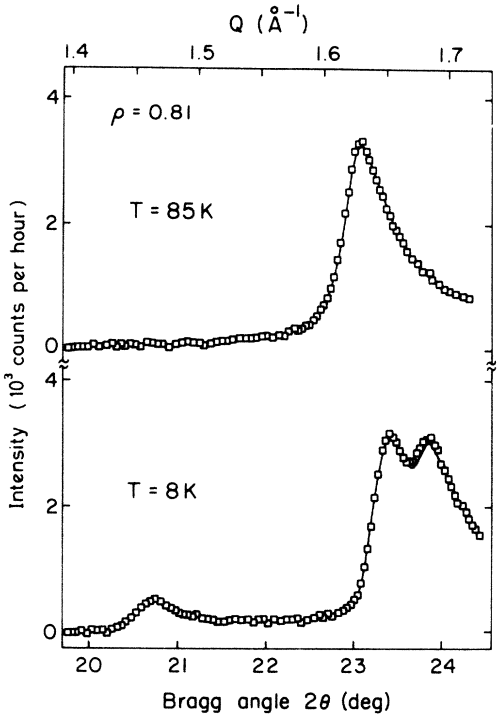

FIG. 2. Diffraction profiles of CF_3H physisorbed on graphite for a coverage of $\rho=0.81$. The background counting rate is subtracted. The 85-K profile shows the triply degenerate (11),(1$\bar{1}$),(02) reflection. At $T=8$ K this reflection splits into the doubly degenerate (11),(1$\bar{1}$) low-angle, and the (02) high-angle, component. An extra (10) reflection appears at $2\theta\approx20.7$ deg.

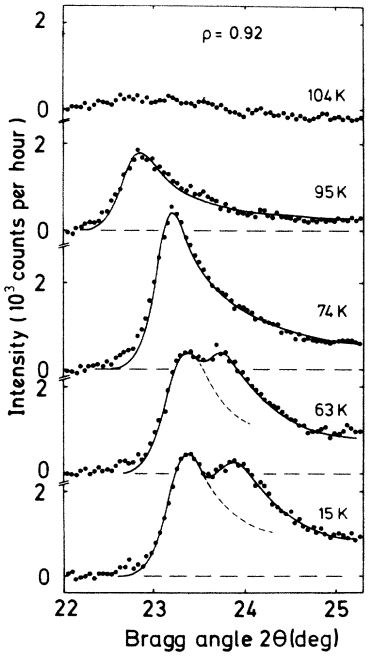

FIG. 3. T dependence of the principal Bragg reflection (11),(1$\bar{1}$),(02), $\rho=0.92$, showing the peak splitting in the low-T phase. Lines are best fits of a Warren profile to the data.

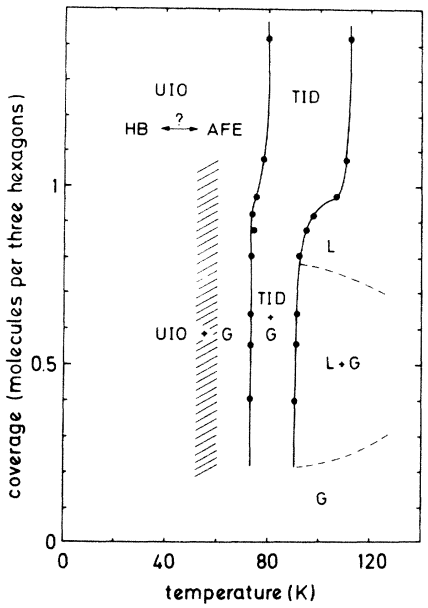

FIG. 4. The temperature-coverage phase diagram of CF_3H adsorbed on graphite. Solid dots mark the transitions actually observed in the diffraction study. L represents liquid; G represents gas; TID represents triangular, incommensurate, orientationally disordered; UIO represents uniaxially compressed, incommensurate, orientationally ordered, HB represents herringbone structure; and AFE represents antiferroelectric structure. The exact extension of the L + G range is unknown. The hatched area indicates the temperature range, where an ordering of perpendicular components of the dipole moments is presumed.

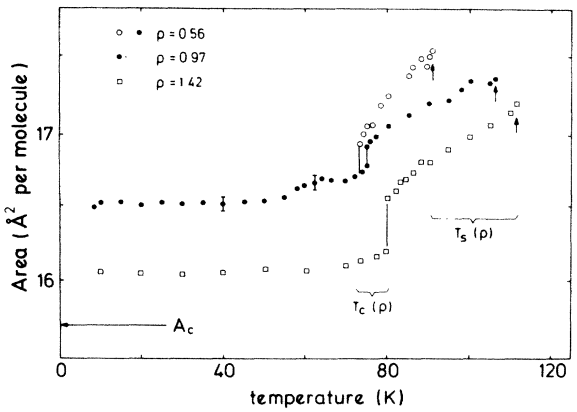

FIG. 5. The temperature dependence of the area per molecule ($A = \frac{1}{2}ab$) for three coverages in the triangular phase ($T_c < T < T_s$) and the ordered phase ($T < T_c$). Vertical lines mark the transition temperatures of the structural transition at T_c, arrows the melting temperature T_s of the 2D solid. A_c is the area of three graphite hexagons, which is the area per molecule in a $\sqrt{3}\times\sqrt{3}$ structure.

angular phase, coherence lengths ξ between 250 and 300 Å have been derived from the fits (solid curves of Fig. 3), values which compare favorably with the intrinsic coherence length of Papyex.[20]

The peak splitting below T_c is due to a compression of the rectangular cell along the b direction, the low-2θ component is identified as (11),(1$\bar{1}$), the high-2θ one as (02). The appearance of the extra (10) line shows that the cell is no longer centered due to staggered internal displacements, respectively orientations. The cell parameters are presented in terms of the area per molecule, A (Fig. 5) and the strain order parameter of the uniaxial compression in terms of $1-b/\sqrt{3}a$ (Fig. 6). Clearly the structural phase transition at T_c is of first order as can be seen from the discontinuities at T_c. The two components of the split reflection are both individually broader than the parent reflection of the triangular phase. For simplicity we have described this broadening by a reduced coherence length in the fits. Values of 220±30 Å for (11),(1$\bar{1}$) and 150±30 Å for (02) have been derived. Presumably the line broadening indicates that facets of the substrate exist which carry more than one domain.

B. Molecular orientation

As usual in diffraction studies on adsorbed monolayers, the experimental information is insufficient for a rigorous structure determination. In particular the diffracted intensity hardly depends on the out-of-plane coordinate of the atomic positions. Hence the arrangement of the molecules has to be inferred from the cell dimensions combined with steric considerations. In the following the orientation of the molecules with respect to the substrate will be specified by the angle α between the surface normal and the C—H bond, to which the electric dipole moment is parallel, and the azimuth φ.

The triangular structure of the high-temperature phase imposes restrictions on the orientations of the molecules. The molecules can be orientationally ordered, with α be-

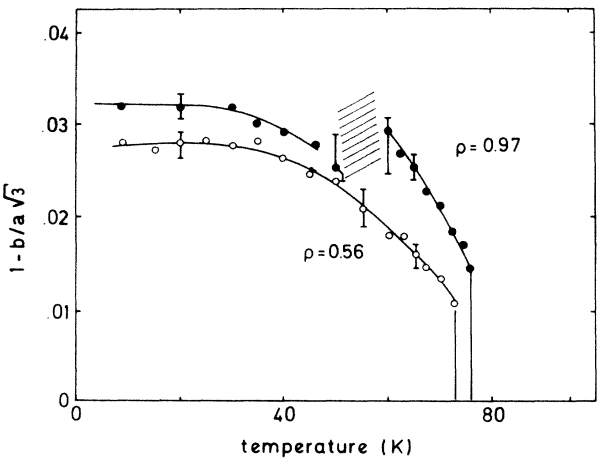

FIG. 6. The temperature dependence of the spontaneous uniaxial strain $1-b/\sqrt{3}a$ of the ordered phase. Solid curves are guides to the eye. The hatched area indicates a T range where the splitting of the principal Bragg reflection is not well determined. a and b are the parameters of the rectangular cell containing two molecules.

ing 0 deg or 180 deg, or orientationally disordered. The case $\alpha=180$ deg, where the molecules stand on the H monopod, is unlikely for energetic reasons. For $\alpha=0$ deg the molecules rest on the F_3 tripod, analogous to CF_4 molecules adsorbed on graphite. For CF_4 the area per molecule, A, ranges from about 19.5 $Å^2$ to 20.9 $Å^2$ (the latter value refers to the 2×2 commensurate phase). In the triangular phase of CF_3H the maximum value of A is 17.5 $Å^2$, only. We conclude that the CF_3H molecule cannot rest on the F_3 tripod but rather has the short extension, which is along the C—H bond, roughly parallel to the surface ($\alpha=90$ deg). For this situation to be compatible with the triangular symmetry, the φ component of the orientation must be disordered. The large thermal contraction observed in this phase supports the idea of thermally activated reorientations with respect to the azimuth φ and of large amplitude α librations. Figure 7(a) shows the triangular arrangement. The molecules are represented by their gyration circle which is estimated from molecular data.[21,22] The strong overlap of these circles proposes that the azimuthal rotation is hindered rather than free involving correlated motions of the neighboring molecules.

As T decreases, the triangular lattice contracts, the φ reorientations become less frequent, and the α amplitudes smaller; finally at T_c the molecules lock in at special φ orientations and the lattice responds by a spontaneous compression. The isotropic and uniaxial component of this compression are shown in Figs. 5 and 6. Based on the cell and the molecular dimensions, two azimuthal arrangements are proposed for the low-temperature phase in Figs. 7(c) and 7(d). (Possible α values will be discussed below.) The molecules are represented by the projections of the two lower F and the H atom onto the surface. The third F and the C atom are omitted for clarity. In both structures the surface is tightly covered with molecules. They have in common the staggered φ arrangement and the off-center position of the second molecule of the cell which is now at the reduced coordinates $x_0,\frac{1}{2}$ as compared to $\frac{1}{2},\frac{1}{2}$ in the triangular phase. The structure of Fig. 7(d) has an in-plane antiferroelectric (AFE) moment, with $\varphi=0$, respectively, $\varphi=180$ deg, and $x_0=0.3$, the electric quadrupole moments being all parallel (ferroquadrupolar). The azimuth φ is counted from the a axis. The herringbone (HB) structure of Fig. 7(c), with $\varphi=60$ deg, respectively, $\varphi=120$ deg, and $x_0=0.75$ can be regarded as a canted ferroelectric and antiferroquadrupolar arrangement of the in-plane moments. The values for φ and x_0 have been simply determined from graphical trial and error by minimizing the overlap between the molecules. Here we noted a high correlation between the azimuth φ and the off-center parameter $(x_0-\frac{1}{2})$, a fact which suggests that the low-temperature phase results from the condensation of a coupled rotational-translational mode at the (10) zone boundary point which is driven by short-range steric interactions. In these terms the (10) intensity should be regarded as a measure of the primary order parameter. Its T dependence is shown in Fig. 8. Note from the inset that the (10) point represents modes with the wavelength $\lambda=|\mathbf{b}|$ traveling along $\mathbf{b}$. As will be pointed out below, there is some indication that just below T_c there is still no ordering of the perpendicular components of the electric dipole moments.

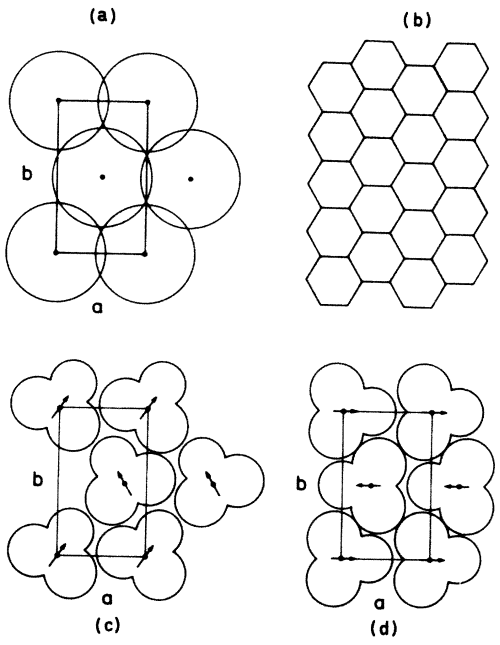

FIG. 7. (a) Upper left: the structure of the disordered phase. The molecules are represented by their gyration spheres. (b) Upper right: the honeycomb lattice of the graphite (001) plane. (c) Lower left: the herringbone structure. (d) Lower right: the antiferroelectric structure. In (c) and (d) the in-plane components of the electric dipole moments are ordered. The molecules are represented by the F_2H contour and the electric dipole vector. The molecules have been drawn to scale by projection using the values known for the van der Waals radii (Ref. 21) and the bond lengths (Ref. 22).

Deciding whether the low-T phase has the antiferroelectric or the herringbone structure should in principle be possible from an analysis of the Bragg intensities. Calculations of the structure factors show that the intensities of the extra reflections are almost identical for the two structures but that the intensity ratio of the two components of the split principal reflection, $(11),(1\bar{1})$ with respect to (02), is about 4 for the AFE and about 0.5 for the HB structure, though one should realize that these values are very sensitive to the exact value of the parameter x_0 and that temperature factors have not been included. The experimental value for the intensity ratio is always 2 ± 0.4 independent of T and ρ, as if the peak would just split without major changes of the structure factor. We conclude that a considerable amount of disorder is carried over from the high-temperature to the low-temperature phase. In fact, a high density of vortex-antivortex defect pairs might blur the difference between the two phases, as has been argued for O_2 monolayers.[10]

A point which should be considered in discussing the low-temperature structure are recent dielectric measurements on CF_3H adsorbed on the (001) faces of BN, which are isomorphous to those of graphite. Several anomalies

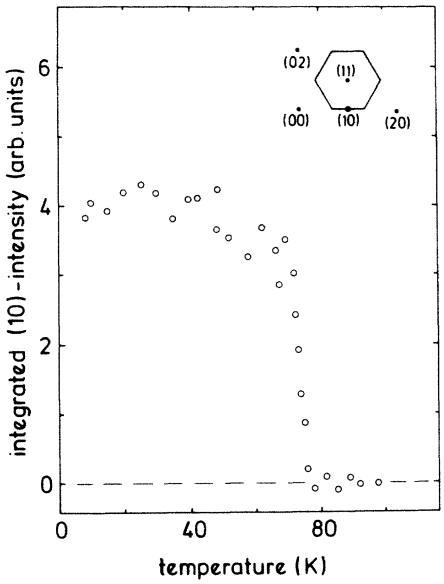

FIG. 8. The temperature dependence of the integrated intensity of the (10) superlattice reflection for $\rho=0.92$. The inset shows a part of the reciprocal lattice including the (11) Brillouin zone and the (10) zone boundary point.

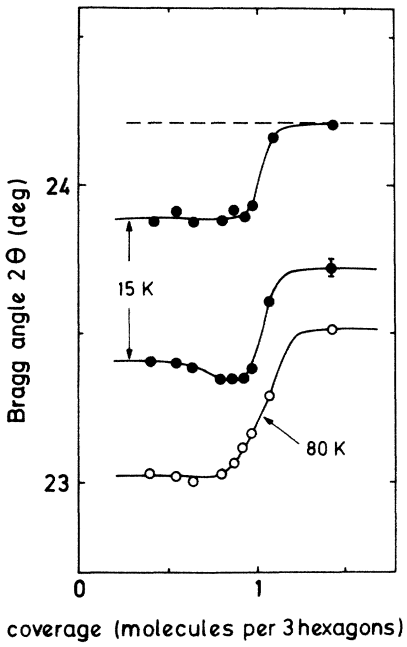

FIG. 9. The dependence of Bragg positions on the coverage. ●, position of the two components of the split principal reflection of the ordered phase at 15 K; ○, position of the principal reflection of the triangular phase at 80 K. Solid curves are guides to the eye. The dashed line indicates the position of the principal reflection of a $\sqrt{3}\times\sqrt{3}$ structure.

of the dielectric response, $\epsilon'(T)$ and $\epsilon''(T)$, have been observed.[17] The temperatures of the weaker ones agree with the phase boundaries $T_s(\rho)$ and $T_c(\rho)$ of the present study, showing that the adsorption behavior of CF_3H on graphite and BN is practically identical. The strongest anomaly, which occurs around 50 K, is reminiscent of the divergent electric response at ferroelectric phase transitions of 3D systems. Hence it is likely that further orientational, ferroelectric-type ordering takes place around 50 K which presumably involves the perpendicular components of the electric dipole moments. One might think, for example, that above 50 K the average α value is still about 90 deg and that below 50 K the molecules settle on their F_2H tripods. Two subtle features of the present diffraction data, which are on the borderline of what can be extracted, actually suggest that a further transition occurs between 50 and 60 K in CF_3H on graphite: a small contraction in $A(T)$ (Fig. 5) and a somewhat diffuse (11),(1$\bar{1}$),(02) splitting in this T range (Fig. 6) for coverages close to $\rho=1$. (In fact, the weakness of these effects supports the idea that the ordering involves perpendicular components only.)

In any case, the low-T phase shows a staggered arrangement of the in-plane moments forming a rectangular lattice, uniaxially compressed with respect to the triangular high-T phase. There are indications for a subsequent ordering of the perpendicular components.

C. Commensurability

An important distinction of adsorbed layers is whether they are incommensurate or commensurate to the substrate corrugation. CF_3H submonolayers are incommensurate, the cell dimensions being intermediate to the $\sqrt{3}\times\sqrt{3}$ and the 2×2 commensurate structures. As demonstrated in Fig. 5, the area per molecule, A, exceeds the area of three graphite hexagons, A_c, for all ρ and T though the mismatch between A and A_c is reduced by the contraction of the lattice at T_c. For coverages $\rho>1$ commensurability is reached in one direction, along b but not along a (Fig. 9). In such a situation a striped pattern of commensurate and incommensurate regions parallel to the b direction is likely. In the submonolayer regime where commensurability is not realized in either direction, the proximity of the $\sqrt{3}\times\sqrt{3}$ structure may nevertheless influence the ordering of the low-T phase via restrictions imposed on the patterns of the orientational domains.

D. Phase diagram

The phase diagram is shown in Fig. 4. The solid dots indicate transitions actually observed in the diffraction experiments. In the submonolayer region where T_s and T_c are independent of the coverage ρ, $T_s(\rho)$ and $T_c(\rho)$ have to be regarded as triple lines; $T_s(\rho)$, for example, separates the liquid-gas (L + G) coexistence range from the gas-triangular solid coexistence range (TID + G), where TID means triangular, incommensurate, and orientationally disordered, as shown in the figure. The shape of the liquid-gas region is hypothetical; the critical point terminating this region is not known. As suggested by the fact that the coherence length of the Bragg peaks of the triangular phase is just equal to the intrinsic coherence length of the substrate, the gas-triangular solid coex-

istence should be understood as a coexistence of graphite facets covered by the solid with those covered by the 2D gas. Presumably the same picture holds for the coexistence region of the gas and the uniaxially compressed phase, but here it may happen that two or more domains coexist on a covered facet. For $0.8<\rho<1.1$, T_c and, in particular, T_s increase with increasing coverage. It is in the same range of coverages that the solid phases contract (Fig. 9). The increase of the transition temperature and the contraction are smaller in the low-T phase which is already more closely packed than in the high-T disordered phase. For $\rho>1.1$, $T_s(\rho)$ is 112 K and presumably identical to the triple point temperature of bulk CF_3H. For bulk CF_3H a value of 118 K has been reported[23] with a deviation of up to 8 K between different references. We observed a freezing temperature of bulk CF_3H of 117 K in our diffraction study and of 116 K in the dielectric measurements. From the observation of the 3D Bragg peaks for $\rho>1$ we conclude that not more than one solid monolayer can be adsorbed before bulk crystallization sets in.

In the low-temperature 2D solid the arrangement of the in-plane components of the electric dipole and quadrupole moments can be of the HB or of the AFE type or of some intermediate case which could be visualized as, say, an AFE structure with a high density of topological faults, vortex-antivortex pairs, or domain boundaries. The intensity ratio of the two components of the split principal reflection favors such a defect-dominated arrangement. The perpendicular components presumably order in a ferroelectric way at temperatures somewhat below T_c as indicated by the hatched range of Fig. 4.

IV. DISCUSSION

In the following we compare the present results to CF_4 and O_2 adsorbed on graphite, the systems to which the closest analogies exist. CF_4 has molecular dimensions almost identical to CF_3H; thus one expects that the 2D phase diagrams resemble each other closely. A number of 2D solid phases have been identified for CF_4 on graphite.[8,9] Apart from a triangular incommensurate solid at higher coverages, a triangular commensurate 2×2 phase has been observed which undergoes two successive transitions into a uniaxially deformed phase and a "three-peak phase" at lower temperatures and appropriate coverages. Another phase may exist between the uniaxially deformed and the "three-peak phase."[9] It is plausible that the nontriangular phases are orientationally ordered. In the uniaxially deformed phase, $b>\sqrt{3}a$, the commensurability to the substrate is maintained in one direction. In this situation striped patterns of domain walls were expected. The theoretical efforts start out from the 2×2 phase which can be equivalently described in terms of a Heisenberg system which face oriented cubic anisotropy.[24] The transitions out of this phase are strongly determined by two types of topological defects, domain walls and dislocations.[25]

The area per molecule is somewhat smaller for CF_3H than for CF_4; hence the commensurability to the substrate is lost and the structures of CF_3H are mainly determined by intermolecular interactions, direct multipolar interactions, and short-range steric repulsion. A modeling in terms of a 2D effective spin Hamiltonian of anisotropic XY form seems more appropriate.[10] Thus, in spite of the similarities of the molecules, the comparison of the two species is not very fruitful. In fact, O_2 on graphite is a more useful reference.

Recent computer simulations[10,12,13] have shown that a structural phase transition should occur for O_2 submonolayers in the δ phase, where the O_2 molecules lie flat on the graphite substrate. At high temperatures the molecules are predicted to form a triangular, orientationally disordered 2D solid; by means of a discontinuous transition orientational order is achieved at lower T.[10] The molecules are now all parallel; the structure can be described by a centered rectangular unit mesh, which is uniaxially distorted ($b>\sqrt{3}a$), giving the low-T phase a ferroquadrupolar and ferroelastic aspect. Both phases are incommensurate. However, there is no experimental evidence to support these results. Low-energy electron diffraction[4,5] (LEED) and x-ray diffraction studies[2] have characterized the δ phase by a centered parallelogram unit cell, slightly distorted from the centered rectangular structure, with the molecules lying parallel to each other and to the surface. The melting occurs at low coverages at $T=26$ K directly from this phase without showing any further transition to an incommensurate triangular orientationally disordered solid phase. As far as the quadrupolar and electric ordering is concerned, there is a closer analogy of the computer-simulation results[10,12,13] to the present system.

CF_3H carries of course an additional electric dipole moment; its quadrupole moment is definitely much smaller than that of O_2. Thus it is not surprising that the ferroquadrupolar order parameter $1-b/a\sqrt{3}$ of CF_3H is reversed in sign and one order of magnitude smaller than in the calculations of Tang *et al.*,[10] which are meant to describe O_2. Nevertheless the theoretical insights which have been obtained for O_2 layers,[10] represented by a two-dimensional planar spin system, should be applicable to the present system. Molecular dynamics revealed that the HB structure and the ferroquadrupolar phase (where the latter one plays the role of the AFE phase of the present system) have almost identical energies, that in fact vortex-antivortex pairs change the structure locally from ferroquadrupolar to HB.[10] The first-order character of the phase transition is caused by a large number of these local defects. A recent Monte Carlo study of an XY antiferromagnet on a 2D triangular lattice demonstrates that the Kosterlitz-Thouless–like transition as defined by the dissociation of the dislocation pairs coincides with the conventional Ising-like transition characterized by the proliferation of the orientational domains.[26] Nevertheless translational and orientational order parameters can have a largely different T dependence.[10] We conclude that the frustration inherent to 2D triangular lattices with "antiferromagnetic" intermolecular interactions will necessarily lead to defective structures and that thinking in terms of perfectly ordered lattices is perhaps not very meaningful.

V. SUMMARY

CF_3H adsorbed on graphite forms two, if not three, 2D crystalline phases. The orientationally disordered phase at high temperatures has a triangular structure incommensurate with the substrate. The low-T phase has staggered in-plane molecular orientations and internal displacements; the lattice is compressed, uniaxially as well as isotropically. Two alternative structures are compatible with the diffraction results of the low-T phase, a herringbone and an antiferroelectric structure. There are indications that the system actually exists in an intermediate state with a high degree of disorder. A subsequent ordering of the perpendicular components of the electric dipoles can be inferred from slight changes of the diffraction pattern in combination with the information from a dielectric study on CF_3H on BN.[17] Above the monolayer completion the growth of bulk crystallites sets in.

ACKNOWLEDGMENTS

We thank M. L. Klein for an enlightening discussion. This work was funded in part by the German Federal Minister of Research and Technology (BMFT) under the Contract No. 05 353 AAI2.

[1]See, e.g., *Ordering in Two Dimensions,* Proceedings of an International Conference held at Lake Geneva, Wisconsin, edited by S. K. Sinha (North-Holland, New York, 1980).

[2]P. A. Heiney, P. W. Stephens, S. G. J. Mochrie, F. Akimitsu, R. F. Birgeneau, and P. M. Horn, Surf. Sci. **125**, 539 (1983).

[3]S. G. J. Mochrie, M. Sutton, J. Akimitsu, R. J. Birgeneau, P. M. Horn, P. Dimon, and D. E. Moncton, Surf. Sci. **138**, 599 (1984).

[4]M. F. Toney, R. D. Diehl, and S. C. Fain, Phys. Rev. B **27**, 6413 (1983).

[5]S. C. Fain, M. F. Toney, and R. D. Diehl, in *Proceedings of the Ninth International Vacuum Congress and Fifth International Conference on Solid Surfaces, Madrid, 1983,* edited by J. L. de Segovia (Imprenta Moderna, Madrid, 1983), p. 129.

[6]J. K. Kjems, L. Passell, H. Taub, J. G. Dash, and A. D. Novaco, Phys. Rev. B **13**, 1446 (1976).

[7]R. D. Diehl and S. C. Fain, Surf. Sci. **125**, 116 (1983).

[8]K. Kjaer, M. Nielsen, J. Bohr, H. J. Lauter, and J. P. McTague, Phys. Rev. B **26**, 5168 (1982).

[9]Q. M. Zhang, H. K. Kim, and M. H. W. Chan, Phys. Rev. B **34**, 8050 (1986).

[10]S. Tang, S. D. Mahanti, and R. K. Kalia, Phys. Rev. Lett. **56**, 484 (1986).

[11]O. G. Mouritsen and A. J. Berlinsky, Phys. Rev. Lett. **48**, 181 (1982).

[12]K. Flurchick and R. D. Etters, J. Chem. Phys. **84**, 4657 (1986).

[13]O. M. B. Duparc and R. D. Etters, J. Chem. Phys. **86**, 1020 (1987).

[14]S. Ostlund and B. I. Halperin, Phys. Rev. B **23**, 335 (1981).

[15]E. Domany and E. K. Riedel, Phys. Rev. B **19**, 5817 (1979).

[16]S. Tang, S. D. Mahanti, and R. K. Kalia, Phys. Rev. B **32**, 3148 (1985).

[17]H. Wiechert, E. Maus, and K. Knorr, Jpn. J. Appl. Phys. **26**, Suppl. 26–3, 889 (1987); and (unpublished).

[18]P. W. Stephens, P. A. Heiney, R. F. Birgeneau, P. M. Horn, D. E. Moncton, and G. S. Brown, Phys. Rev. B **29**, 3512 (1984).

[19]N. Dupont-Pavlovsky, C. Bockel, and A. Thomy, Surf. Sci. **160**, 12 (1985).

[20]R. J. Birgeneau, P. A. Heiney, and J. P. Pelz, Physica **109&110** B, 1785 (1982).

[21]S. C. Nyburg and C. H. Faerman, Acta Crystallogr., Sect. B **41**, 274 (1985).

[22]*Structure Data of Free Polyatomic Molecules,* Vol. 7 of *Landolt-Börnstein,* edited by K.-H. Hellwege and A. M. Hellwege (Springer-Verlag, Berlin, 1976), Vol. 7, p. 124.

[23]*Wärmetechnische Messverfahren, Thermodynamische Eigenschaften Homogener Stoffe,* Vol. IV of *Landolt-Börnstein,* edited by H. Hausen (Springer-Verlag, Berlin, 1967), Part 4a, p. 753.

[24]M. Schick, Surf. Sci. **125**, 94 (1983).

[25]P. Bak and T. Bohr, Phys. Rev. B **27**, 591 (1983).

[26]J. E. Van Himbergen, Phys. Rev. B **33**, 7857 (1986).